Please cite this article as: Finnegan W., Goggins J., 'Linear irregular wave generation in a numerical wave tank'. *Applied Ocean Research* 52 (2015) 188–200. DOI:10.1016/j.apor.2015.06.006

Linear irregular wave generation in a numerical wave tank

William Finnegan[a,b], Jamie Goggins[a,b,c,*]

[a] *College of Engineering and Informatics, National University of Ireland, Galway, Ireland*
[b] *Ryan Institute for Environmental, Marine and Energy Research, National University of Ireland, Galway, Ireland*
[c] *Marine Renewable Energy Ireland (MaREI) Research Centre, Galway, Ireland*
***** *Tel: +35391492609, Fax: +35391494507, E-mail: jamie.goggins@nuigalway.ie*

Abstract

In the design of any floating or fixed marine structure, it is vital to test models in order to understand the fluid/structure interaction involved. A relatively inexpensive method, compared to physical model testing, of achieving this is to numerically model the structure and the wave conditions in a numerical wave tank. In this paper, a methodology for accurately replicating measured ocean waves in a numerical model at full scale is detailed. A Fourier analysis of the measured record allows the wave to be defined as a summation of linear waves and, therefore, Airy's linear wave theory may be used to input the wave elevation and associated water particle velocities. Furthermore, a structure is introduced into the model to display the ability of the model to accurately predict wave-structure interaction. A case study of three individual measured waves, which are recorded at the Atlantic marine energy test site, off the west coast of Ireland, is also presented. The accuracy of the model to replicate the measured waves and perform wave-structure interaction is found to be very high. Additionally, the absolute water particle velocity profile below the wave from the numerical model is compared to a filtered analytical approximation of the measured wave at a number of time steps and is in very good agreement.

Keywords: *ANSYS CFX, Computational fluid dynamics, Linear irregular waves, Wave energy, Wave-structure interaction.*

Please cite this article as: Finnegan W., Goggins J., 'Linear irregular wave generation in a numerical wave tank'. *Applied Ocean Research* 52 (2015) 188–200. DOI:10.1016/j.apor.2015.06.006

1. Introduction

In real ocean conditions the waves are not linear or even regular in form. Therefore, it is necessary to develop a method of generating a wave which accurately represents real sea conditions. In general, when a measuring wave buoy records a wave, the wave energy spectrum is generated for that record and over time a catalogue of wave energy spectra are analysed for that site to formulate a single wave energy spectrum which is used to represent the wave climate of a given sea or ocean region. From this spectrum, a Fourier transform may be used to derive an irregular linear wave profile which represents typical waves at the location.

In this study, measured wave elevation records from a location are used and recreated. The main principle being used is the theory that real ocean waves are accurately represented by a linear irregular wave. However, these generated waves may not be an accurate representation of the typical wave climate but are, in fact, replications of real measured records. In other words, single samples are analysed and replicated and are not representative of the long-term wave climate. A major advantage of this is that extreme or exceptional wave conditions recorded at a location can be recreated accurately.

Various numerical modelling techniques, such as the boundary element method (BEM) [2, 4, 9, 12, 15, 18], finite element method (FEM) [3] and finite volume method (FVM) [5, 11, 13, 14, 16, 17], can be employed to represent linear irregular waves and nonlinear motions of floating bodies in water. A summary of selected relevant publications which explore wave generation and wave-structure interaction, particularly concerning irregular wave generation, are presented in . The commercial software packages used to implement the study are specified. However, where in-house software code was used, no software package is specified.

Please cite this article as: Finnegan W., Goggins J., 'Linear irregular wave generation in a numerical wave tank'. *Applied Ocean Research* 52 (2015) 188–200. DOI:10.1016/j.apor.2015.06.006

Table 1: Summary of selected publications (including present study) detailing wave generation and wave-structure interaction

Reference	Numerical method	Commercial software package	Reg/Irr waves	Wave generation method	Nonlinear waves	Wave-structure interaction
Kim et al. [1]	FDM	-	Reg, Irr	Flap-type wavemaker	✓	-
Boo [2]	HOBEM	-	Reg, Irr	Numerical	✓	✓
Turnbull et al. [3]	FEM	-	Reg	Numerical	✓	✓
Koo and Kim [4]	BEM	-	Reg	Numerical	✓	✓
Park et al. [5]	FVM	-	Reg, Irr	Numerical	✓	✓
Wu and Hu [6]	FEM	-	Reg, Irr	Piston-type wavemaker	✓	✓
Hadzic et al. [7]	-	Comet	-	Numerical	✓	✓
Sriram et al. [8]	FEM	-	Reg, Irr	Piston-type wavemaker	✓	-
Ning and Teng [9]	HOBEM	-	Reg, Irr	Numerical	✓	-
Agamloh et al. [10]	-	Comet	Reg, Irr	Piston-type wavemaker	✓	✓
Lal and Elangovan [11]	FVM	ANSYS CFX	Reg	Flap-type wavemaker	-	-
Ning et al.[12]	HOBEM	-	Reg	Numerical	✓	-
Liang et al. [13]	FVM	FLUENT	Irr	Piston-type wavemaker	✓	-
Elangovan [14]	FVM	ANSYS CFX	Irr	Flap-type wavemaker	-	-

Please cite this article as: Finnegan W., Goggins J., 'Linear irregular wave generation in a numerical wave tank'. *Applied Ocean Research* 52 (2015) 188–200. DOI:10.1016/j.apor.2015.06.006

Yan and Lui [15]	HOBEM	-	Reg	Numerical	✓	✓
Finnegan and Goggins [16]	FVM	ANSYS CFX	Reg	Flap-type wavemaker	-	✓
Yu and Li [17]	FVM	STAR-CCM+	Reg	Numerical	-	✓
Present study	*FVM*	*ANSYS CFX*	*Irr*	*Numerical*	-	✓

Legend: BEM: boundary element method, FDM: finite difference method, FEM: finite element method, FVM: finite volume method, HOBEM: higher-order boundary element method, Irr: irregular waves studied, Reg: regular waves studied.

In recent years, a number of studies were performed using commercial software packages (see), where are based on the Reynolds averaged Navier-Stokes equations. For example, Lal and Elangovan [11] explored the CFD simulation of linear water waves for a flap type wavemaker using the same finite volume package described in this study. However, the dimension of the model was taken as an experimental wave tank and simulations were only carried out for the shallow water case. Finnegan and Goggins [16] presented a methodology for developing an optimum numerical wave tank model which can accurately generate linear water waves and perform wave-structure interaction. In this methodology, the overall dimensions, the model mesh, the time-step and the method of wave energy dissipation at the end of the model are analysed and optimised. Yu and Li [17] used a Reynolds averaged Navier-Stokes based CFD method to explore the relative response of a two-body floating-point absorber in linear regular waves, in terms of its power generation capacity. Liang et al. [13] explored the use of a piston type wavemaker to generate an irregular wave train using the finite volume method, using FLUENT, and compared the results to the results from that of an experimental wave tank. Elangovan [14] extended the work of Lal and Elangovan [11] to simulate irregular linear waves using a flap-type wavemaker in a wave tank, which is based on an actual experimental wave tank. The method is validated by comparing the output wave spectrum to the original. Agamloh et al. [10] used a commercial CFD software package to develop a 3-D numerical wave tank, which allowed fluid-structure interaction of a water wave and a cylindrical ocean wave energy device to be explored. Both the response of a single device and the response of an array of devices were investigated.

Please cite this article as: Finnegan W., Goggins J., 'Linear irregular wave generation in a numerical wave tank'. *Applied Ocean Research* 52 (2015) 188–200. DOI:10.1016/j.apor.2015.06.006

In this paper, a CFD numerical wave tank model, developed using the commercial finite volume method package ANSYS CFX, is presented for replicating measured real ocean waves at full scale. The fast Fourier transform is utilised in order to create an input wave, together with its associated water particle velocities, which replicates a measured wave record. The wave was recorded at the Atlantic marine energy test site (AMETS) [54.225N, -9.991W], as shown in Figure 1. Three different wave records are replicated and compared with the measured wave in the time domain, as well as their corresponding wave energy spectra. Additionally, the absolute water particle velocity profile below the wave from the numerical model is compared to the filtered analytical approximation of the measured wave. Furthermore, a rectangular prism structure is introduced into the model in order to explore the interaction between a linear irregular ocean wave and a structure. The dynamic response of the structure to the linear irregular wave is compared with the analytical prediction, which is derived from a hydrodynamic analysis.

Figure 1: Map showing the location of the wave data buoy at AMETS, Ireland. Adapted from: [19]

Please cite this article as: Finnegan W., Goggins J., 'Linear irregular wave generation in a numerical wave tank'. *Applied Ocean Research* 52 (2015) 188–200. DOI:10.1016/j.apor.2015.06.006

2. Methodology

In this section, the methodology for replicating a measured wave in a CFD model is described. Offshore ocean waves are irregular and random in nature with each different to the previous. For the most of the time, offshore ocean waves may be described as linear irregular waves and this is the type of wave which is being detailed in this study. It is acknowledged that when dealing with near-shore waves this is not always true, as a number of significant non-linearities are introduced due to the interaction of the wave with the coastline and the seabed. Similarly, there can be non-linearities associated with extreme wave conditions. However, these scenarios are outside the scope of this study.

The measured wave records, which are to be replicated in this analysis, have been recorded at the Atlantic marine energy test site (AMETS) off Belmullet, Co. Mayo, Ireland [19]. A map detailing the location of the wave data buoy at AMETS, which is located at 54.225N, -9.991W, is shown in Figure 1. AMETS has been selected for the full-scale testing of pre-commercial wave energy devices. The site itself provides facility for the testing of near-shore, intermediate-water and offshore devices. It was selected principally due to its deep water with sandy seabed close to shore, the quality of its wave climate, the onshore infrastructure and the suitable grid connection. A Fugro Wavescan buoy is used to record the real-time wave data and is located approximately 3 km offshore in water depth of 50 to 100m. The measured wave records are taken over a half hour time frame and three records are used in the analysis. Data recorded over two years at AMETS is used in the case study analysis discussed in Goggins and Finnegan [20].

The initial part of the study is to analytically describe the measured wave by using an irregular linear wave, which is comprised of a summation of a number of linear waves. This analytical approximation is then employed in the CFD model, which is implemented in the commercial software package ANSYS CFX [21]. The software uses a finite volume method in order to solve the Reynolds Averaged Navier-Strokes equations (RANSE), which accounts for turbulence and viscosity. Its governing equations are described in Section 2.1. ANSYS CFX offers increased user flexibility, compared to similar commercial codes, with a well-developed graphical user interface

Please cite this article as: Finnegan W., Goggins J., 'Linear irregular wave generation in a numerical wave tank'. *Applied Ocean Research* 52 (2015) 188–200. DOI:10.1016/j.apor.2015.06.006

and the option of an expression language, along with user defined functions written in FORTRAN. Additionally, ANSYS CFX uses a node centered solver, which offers increased accuracy compared to more common cell centered solver. However, since the analysis is performed on an ANSYS academic licence, there are a number of limitations, including the maximum geometry dimension is 500 m and there is a node limit of 512000 nodes, which is approximately 1.2 x 10^6 elements, which restricts the dimension of the fluid domain. In order to replicate the wave accurately at the desired location, an input wave with corresponding water particle velocities is derived and used as the input in the CFD model.

In order to validate the accuracy of the solution, the analytical wave and the output wave from the CFD model are compared in the time-domain. In addition, the wave energy spectrum from the resulting output wave from the CFD model and the wave energy spectrum from the measured data are compared.

The methodology used in this section is similar to that described by Elangovan [14]. However, Elangovan [14] uses a flap-type wavemaker to generate the incident wave, while a numerical input of the wave elevation and the water particle velocities is used in this analysis. One of the major advantages of the numerical input is that computation time is reduced as the initial mesh can be used throughout the analysis as there are no moving boundaries. On the other hand, a wavemaker requires a moving boundary and, thus, remeshing at each time-step.

Finally, a rectangular prism structure is introduced into the model in order to explore the interaction between a linear irregular ocean wave and a structure. This, as is the nature of the problem, will introduce a moving boundary at the structure wall and, in turn, will require extra adaptions to the model to increase its robustness. However, this subject is secondary to the primary study of the paper of linear irregular wave generation and is detailed in Section 4.

2.1 The governing equations

The method on which the solver in ANSYS CFX is based on is the finite volume technique [21]. This technique divides the region of interest into sub-regions and discretises the governing

Please cite this article as: Finnegan W., Goggins J., 'Linear irregular wave generation in a numerical wave tank'. *Applied Ocean Research* 52 (2015) 188–200. DOI:10.1016/j.apor.2015.06.006

equations in order to solve them iteratively over each sub-region. Therefore, an approximation of the value of each variable at points throughout the domain is achieved.

The governing equations that need to be solved by the ANSYS CFX solver is the mass continuity equation [22], which is given as:

$$\frac{\partial \rho}{\partial t} + \frac{\partial \rho u_1}{\partial x} + \frac{\partial \rho u_2}{\partial y} = 0 \tag{1}$$

and the Navier-Stokes equations [22], which are given as:

$$\rho\left(\frac{\partial u_1}{\partial t} + u\frac{\partial u_1}{\partial x} + v\frac{\partial u_1}{\partial y}\right) = -\frac{\partial p}{\partial x} + 2\mu\frac{\partial^2 u_1}{\partial x^2} + \frac{\partial}{\partial y}\left(\mu\left(\frac{\partial u_1}{\partial y} + \frac{\partial u_2}{\partial x}\right)\right) + F_1 \tag{2}$$

$$\rho\left(\frac{\partial u_2}{\partial t} + u\frac{\partial u_2}{\partial x} + v\frac{\partial u_2}{\partial y}\right) = -\frac{\partial p}{\partial y} + 2\mu\frac{\partial^2 u_2}{\partial y^2} + \frac{\partial}{\partial x}\left(\mu\left(\frac{\partial u_1}{\partial y} + \frac{\partial u_2}{\partial x}\right)\right) - \rho g + F_2 \tag{3}$$

where t is time, x is the horizontal distance from the wavemaker, y is the vertical height from the still water level (SWL) and increases with depth, ρ is fluid density, u_1 is the horizontal flow velocity, u_2 is the vertical flow velocity, F_1 is the horizontal force on the fluid, F_2 is the vertical force on the fluid, p is pressure and μ is viscosity.

In order to determine the position of the free surface, or air-water boundary, the volume of fluid method is applied. This technique was also employed by Liang et al. [13]. This method adds another governing equation, given by:

$$\frac{\partial q_i}{\partial t} + u_1\frac{\partial q_i}{\partial x} + u_2\frac{\partial q_i}{\partial y} = 0, i = 1,2 \tag{4}$$

where q_i is the volume fraction of the fluid i with $\sum_{i=1}^{2} q_i = 1$. The free surface is then approximated as at the position of the minimum of value $|q_1 - q_2|$ along the model.

2.2 CFD model set-up

Please cite this article as: Finnegan W., Goggins J., 'Linear irregular wave generation in a numerical wave tank'. *Applied Ocean Research* 52 (2015) 188–200. DOI:10.1016/j.apor.2015.06.006

The CFD model set-up used in this analysis is mainly based on the methodology described in Finnegan and Goggins [16]. The set-up for the CFD model is divided into three stages: (1) the geometry setup, which defines the physical dimensions of the model, (2) the mesh setup, where the computational domain mesh is created and (3) the wave-water, or physics, setup, which defines the analysis type, the domain setup, the boundary conditions, the initial water height and other characteristics of the water and air-water interaction.

2.2.1 Model geometry

A 3-D geometry of the model is used with a thickness less than the size of an element. However, two symmetry boundaries are utilised, so the numerical model is infinitely wide. Since the maximum dimension, as a result of a limitation in the ANSYS academic licence, is 500 m, the total length of the model is 500 m and total height of 100 m, with a SWL of 70 m.

2.2.2 Mesh refinement and set-up

Since the volume of fraction method is used to define the water level, it is necessary to refine the mesh at the SWL in order to capture the free surface accurately, which is shown in Figure 2. This technique is similar to that employed by Lal and Elangovan [11], Liang *et al.* [13] and in Finnegan and Goggins [16]. The thickness of the refined mesh at the SWL is dependent on the maximum amplitude of the wave, which is 5m above and below the SWL in this study, with a maximum element size specified. The remainder of the domain has a maximum element size specified. Three types of meshes were investigated with varying levels of refinement: a 10868 element mesh with a domain maximum element size of 3.5 m and an element size of 0.3 m at the SWL; a 16588 element mesh with a domain maximum element size of 3.5 m and an element size of 0.15 m at the SWL; and a 22500 element mesh with a domain maximum element size of 2 m and an element size of 0.3 m at the SWL. However, no significant difference (coefficient of determination, R^2, of 99.8) was observed with the increased refinement and, therefore, the 10868 element mesh is used within the computational domain for all simulations described in this section.

Please cite this article as: Finnegan W., Goggins J., 'Linear irregular wave generation in a numerical wave tank'. *Applied Ocean Research* 52 (2015) 188–200. DOI:10.1016/j.apor.2015.06.006

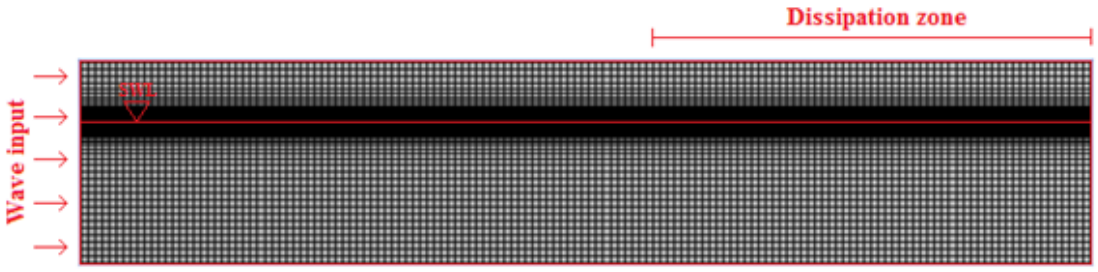

Figure 2: Typical longitudinal elevation of the mesh for CFD model with refinement along the SWL. Included is a schematic of the location of the wave input boundary, the SWL and the dissipation zone.

2.2.3 Pre-solver set-up

In defining the domain set-up, a number of assumptions are included. The surface tension at the air-water interface is assumed to be negligible. An initial hydrostatic pressure is specified in the 'Water' region with no pressure in the 'Air' region and the entire region is static initially. The air is specified to a temperature of 25 °C and, therefore, its density is specified to be 1.185 kg/m^3. Furthermore, an isothermal heat transfer model is specified, which is homogeneous. The fluid (water) temperature is defined as 25°C and its density is given as 1030 kg/m^3 to represent salt water. The dynamic viscosity of the water is 8.899 x 10^{-4} kg/ms for the first 300 m of the model. Then the dynamic viscosity is used to dissipate the energy in the wave, increasing linearly to 125000 kg/ms as it reaches the outflow boundary. Therefore, the dynamic viscosity of the fluid is defined as:

$$\mu = \begin{cases} 8.899 \text{ x } 10^{-4} \text{ kg/ms}, & \text{x} < 300\ m \\ 8.899 \text{ x } 10^{-4} \text{ kg/ms} + \dfrac{\text{x} - 300 \text{ m}}{200 \text{ m}} 125000 \text{ kg/ms}, & \text{x} \geq 300 \text{ m} \end{cases} \quad (5)$$

The top of the model has an *'opening'* boundary condition, which allows air to pass through. At the water inflow boundary, the wave elevation, as well as the horizontal and vertical water particle velocities, needs to be specified. The water inflow boundary is also modelled as an *'opening'* boundary condition, which allows a fluid to cross the boundary in either direction. This type of boundary is necessary at the water inflow boundary when specifying the water particle velocities, which are specified both in and out of the fluid domain, and for allowing any reflected waves from

Please cite this article as: Finnegan W., Goggins J., 'Linear irregular wave generation in a numerical wave tank'. *Applied Ocean Research* 52 (2015) 188–200. DOI:10.1016/j.apor.2015.06.006

inside the computational domain to pass through the boundary without being re-reflected back into the fluid domain, ensuring that the incoming wave will not be affected. An insignificant initial horizontal air velocity is also specified. The volume of fraction is utilised here to differentiate between the *'Water'* velocities and *'Air'* velocities. The details of these inputs are described in more detail in the next section and are inputted using the ANSYS CFX expression language (CEL) [21]. At the outflow boundary there is a hydrostatic pressure specified over the water depth to the initial SWL to allow for overspill of excess water and allow air to pass. There are symmetry boundary conditions specified for the adjacent sides, in order to create a model that is infinitely wide, and the remaining boundaries are assigned a static wall boundary condition.

Previous studies on linear wave generation [11, 16] found that the turbulence model used doesn't affect the generated wave. However, a comparison between three turbulence models was performed in this study in order to investigate if this was also the case for irregular linear wave generation. The three turbulence models investigated are: Laminar, k-epsilon and shear stress transport (SST). The results of the study are presented in Figure 3 and it is evident that the turbulence model used does have an effect on the numerical procedure. Therefore, since the main object of the paper is to generate irregular linear waves, a laminar turbulence model is used throughout the study.

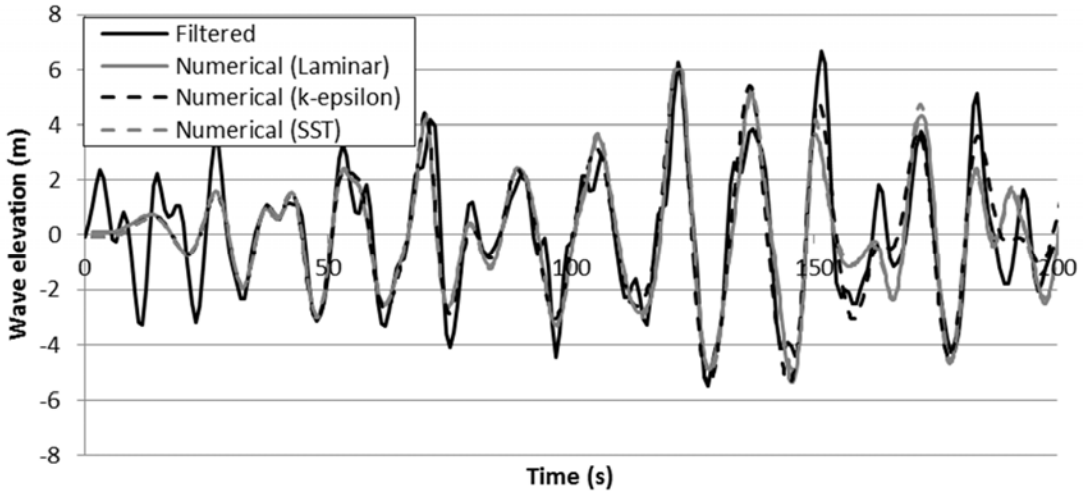

Figure 3: Comparison between the filtered analytical wave and the numerical wave generated using three turbulence models: Laminar; k-epsilon and shear stress transport (SST).

Please cite this article as: Finnegan W., Goggins J., 'Linear irregular wave generation in a numerical wave tank'. *Applied Ocean Research* 52 (2015) 188–200. DOI:10.1016/j.apor.2015.06.006

2.3 CFD input wave

The input wave at the water inflow boundary of the CFD model is in the form of an irregular linear wave. In order to deduce this irregular linear wave, the fast Fourier transform (FFT) is used. Further details on the use of FFT for signal processing and its uses in ocean engineering can be found in Kim [23]. FFT expresses an irregular linear wave elevation, $\eta(t)$, as a summation of sinusoidal components as follows:

$$\eta(t) = \sum_{n=1}^{\infty} \left(\hat{A}_n \cos \omega_n t + \hat{B}_n \sin \omega_n t \right) \tag{6}$$

where

$$\hat{A}_n = \frac{2}{T_{tot}} \int_{-\frac{T_{tot}}{2}}^{\frac{T_{tot}}{2}} \eta(t) \cos \omega_n t \, dt$$

$$\hat{B}_n = \frac{2}{T_{tot}} \int_{-\frac{T_{tot}}{2}}^{\frac{T_{tot}}{2}} \eta(t) \sin \omega_n t \, dt \tag{7}$$

where T_{tot} is the total time of the simulation and ω_n is the wave angular frequency of the n^{th} linear wave. Introducing N number of time-steps, $T_{tot} = N\Delta t$. Therefore, the irregular linear wave elevation may be expressed as:

$$\eta(t_m) = \mathrm{Re}\left[\sum_{n=1}^{N/2} \left(\hat{A}_n - i\hat{B}_n \right) e^{i2\pi f_n t_m} \right], \; m=1,2..N \tag{8}$$

where t_m is the time at the m^{th} time-step and f_n is the frequency of the n^{th} linear wave. Therefore, the Fourier transform, $\hat{X}(f_n)$, is given as:

$$\hat{X}(f_n) = \frac{\hat{A}_n - i\hat{B}_n}{2\pi} \tag{9}$$

And the wave energy spectrum is given as:

Please cite this article as: Finnegan W., Goggins J., 'Linear irregular wave generation in a numerical wave tank'. *Applied Ocean Research* 52 (2015) 188–200. DOI:10.1016/j.apor.2015.06.006

$$S(f_n) = \frac{\left|\hat{X}(f_n)\right|^2}{T_{tot}} \tag{10}$$

However, since Airy's linear wave theory is to be used in the analysis the irregular linear wave elevation has to be rewritten in the form:

$$\eta(t) = \sum_{n=1}^{\infty} \mathrm{A}_n \, cos(-\omega_n t - \varepsilon_n) \tag{11}$$

where

$$\varepsilon_n = \begin{cases} \tan^{-1}\left(\dfrac{-\hat{B}_n}{\hat{A}_n}\right), & \text{for } \hat{A}_n > 0 \\ \pi + \tan^{-1}\left(\dfrac{-\hat{B}_n}{\hat{A}_n}\right), & \text{for } \hat{A}_n < 0 \end{cases} \tag{12}$$

and

$$A_n = \sqrt{2S(f_n)\Delta f_n} \tag{13}$$

where A_n is the wave amplitude of the n^{th} linear wave. Furthermore, in the CFD model, the wave is being replicated at a distance x from the input boundary, so this must be accounted for in the input wave. This is achieved by using the $k_{0,n}x$ term in Eqn. (14), where k_0 is the wavenumber, which is obtained from the relation $\omega^2 = gk_0 tanh\, k_0 h$. In addition, the wave needs to begin at the SWL and increase, so a time offset t' is also introduced. Thus, an adapted phase angle is introduced:

$$\varepsilon_n{}' = \varepsilon_n + k_{0,n}x + \omega_n t' \tag{14}$$

As a result of a limitation with the method of inputting the summation of the wave elevation and water particle velocities into the CFD model, in this analysis, the thirty waves with the highest wave amplitude are taken and, thus, the number of summations, N = 30. Therefore, the wave elevation being inputted into the CFD model is:

$$\eta(t) = \sum_{n=1}^{\mathrm{N}} \mathrm{A}_n \, cos(-\omega_n t - \varepsilon_n{}') \tag{15}$$

Please cite this article as: Finnegan W., Goggins J., 'Linear irregular wave generation in a numerical wave tank'. *Applied Ocean Research* 52 (2015) 188–200. DOI:10.1016/j.apor.2015.06.006

A comparison between the measured wave, where the full 30 minute record is given in Figure 4, and this filtered analytical approximation can be seen in Figure 5. Similar to the approach of Zhao et al. [24], Dong et al. [25] and Xu et al. [26], the horizontal and vertical water particle velocities, along with the wave elevation given in Eqn. (15), are specified at the input boundary. From Airy's linear wave theory, the water particle velocities are given as:

$$u_1(t) = \sum_{n=1}^{\mathrm{N}} \mathrm{A}_n \omega_n \frac{\cosh\left(k_{0,n}\mathrm{y}'\right)}{\sinh\left(k_{0,n}\mathrm{d}\right)} cos(-\omega_n t - \varepsilon_n{}') \tag{16}$$

and

$$u_2(t) = \sum_{n=1}^{\mathrm{N}} \mathrm{A}_n \omega_n \frac{\sinh\left(k_{0,n}\mathrm{y}'\right)}{\sinh\left(k_{0,n}\mathrm{d}\right)} sin(-\omega_n t - \varepsilon_n{}') \tag{17}$$

where $u_1(t)$ and $u_2(t)$ are the horizontal and vertical water particle velocities, respectively, and *y'* is the vertical distance from the base of the model. When entering the water particle velocities at the input boundary, the volume of fluid method (VOF) is utilised to differentiate between the *'Air'* and *'Water'* regions.

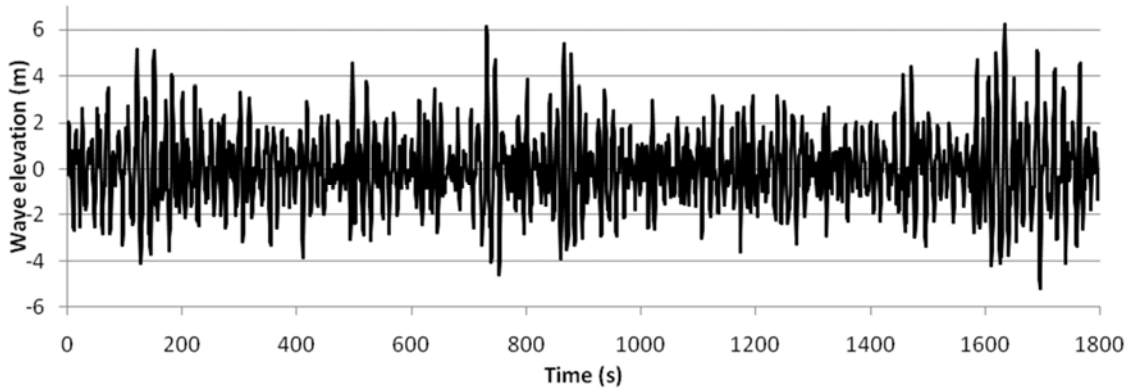

(a)

Please cite this article as: Finnegan W., Goggins J., 'Linear irregular wave generation in a numerical wave tank'. *Applied Ocean Research* 52 (2015) 188–200. DOI:10.1016/j.apor.2015.06.006

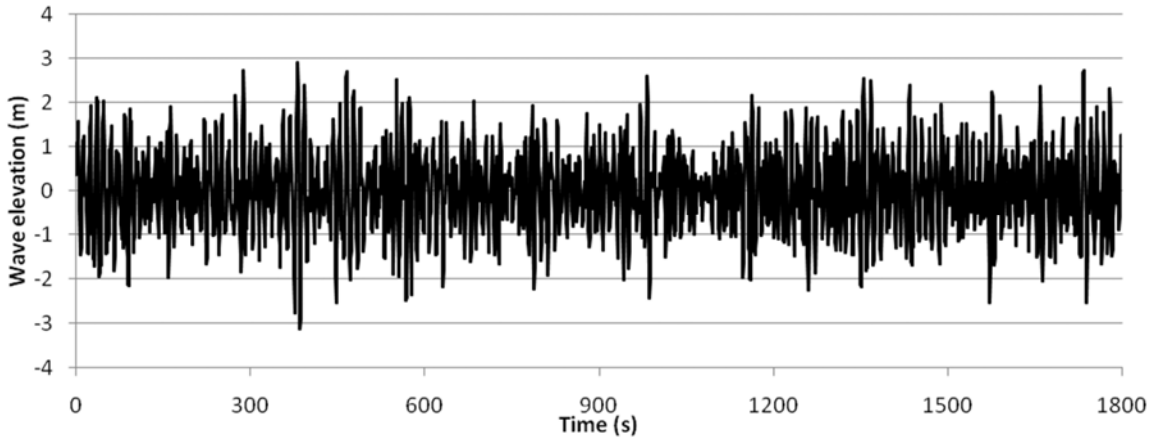

(b)

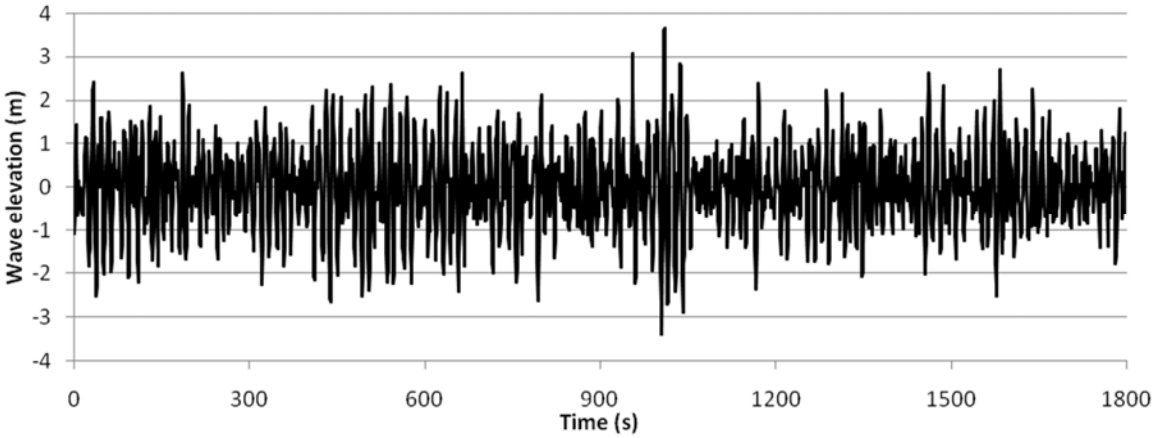

(c)

Figure 4: Measured wave elevation at AMETS beginning at: (a) 10:30 on 17-12-2010 (b) 4:30 on 04-10-2010 and (c) 17:00 on 02-09-2011

3. Results of linear irregular wave generation

In order to validate the integrity of the wave input methodology and the CFD model, described in Section 2, three measured wave records from AMETS are analysed and reproduced numerically. The records are taken on three different days and are 30 minutes in total. These records are

Please cite this article as: Finnegan W., Goggins J., 'Linear irregular wave generation in a numerical wave tank'. *Applied Ocean Research* 52 (2015) 188–200. DOI:10.1016/j.apor.2015.06.006

displayed in Figure 4. However, in this analysis, when comparing the measured and numerical waves, only the first 200 seconds of each record is to be reproduced.

The methodology detailed in Section 2 is then applied to these three 200 s records. The first step is to use the FFT to derive the analytical linear irregular wave approximation, given in Eqn. (11), of the measured wave. As stated earlier, as there is a restraint in the summation of regular waves of N = 30, the 30 highest amplitude regular waves are used to generate the analytical linear irregular wave approximation. The total time of the simulation analysed and replicated is also dependent on the value of N as the measured record is sampled at 1.28 Hz. Therefore, for a 200 s record, the Fourier transform returns 128 waves and this is the limit if only the thirty highest waves are to be replicated. A comparison between the filtered analytical approximation and the measured wave record at AMETS can be seen in Figure 5. It is clear to see, that the approximation slightly over estimates the amplitude of the peaks, but the frequencies match up very well. Therefore, in all three cases, the analytical linear irregular wave approximation provides a very good representation of the measured waves.

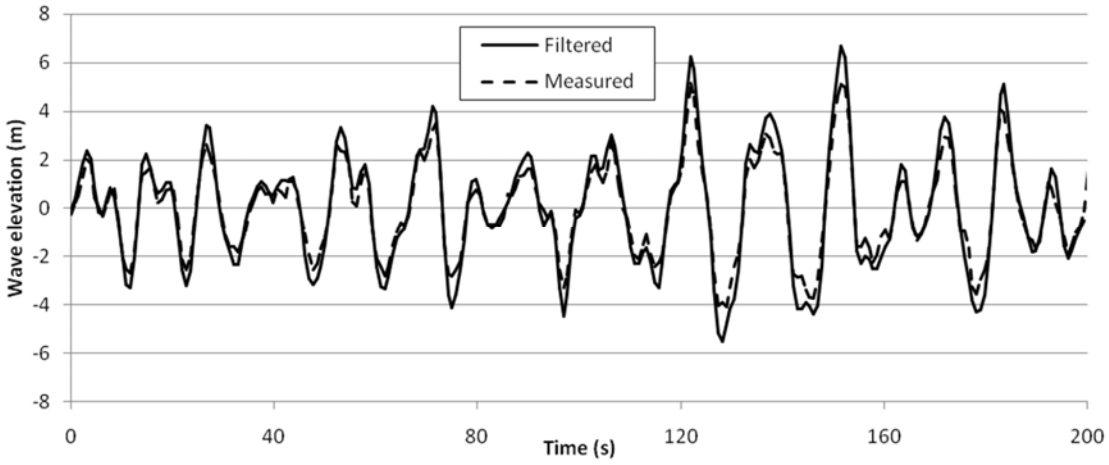

(a)

Please cite this article as: Finnegan W., Goggins J., 'Linear irregular wave generation in a numerical wave tank'. *Applied Ocean Research* 52 (2015) 188–200. DOI:10.1016/j.apor.2015.06.006

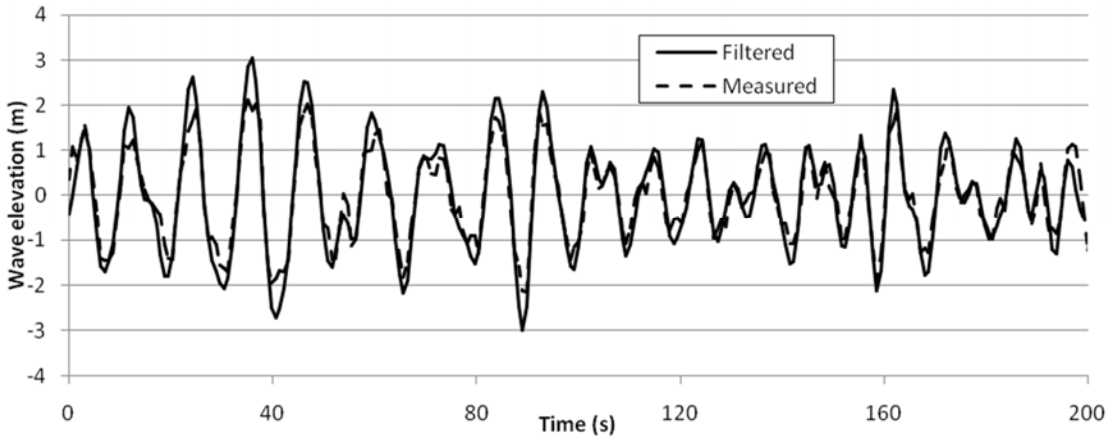

(b)

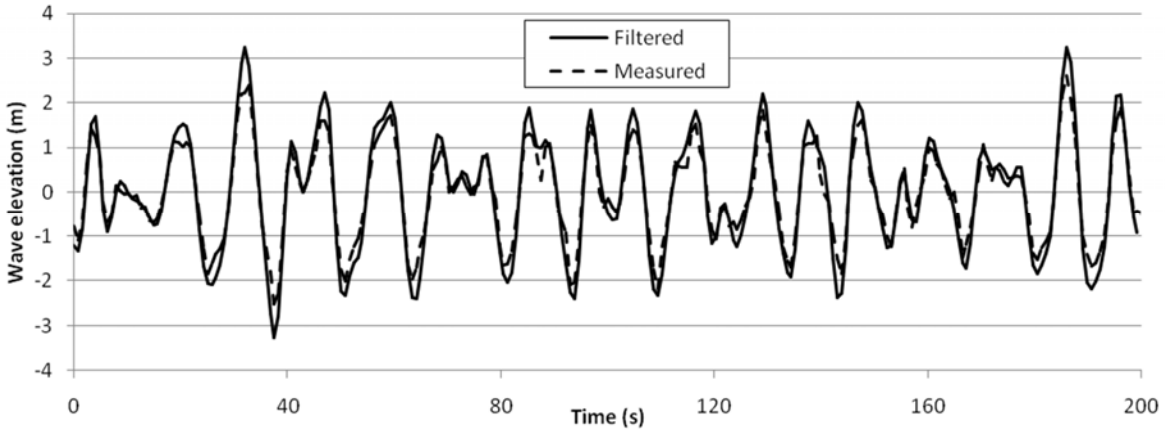

(c)

Figure 5: Comparison between the measured wave at AMETS and the filtered analytical approximation beginning at: (a) 10:30 on 17-12-2010 (b) 4:30 on 04-10-2010 and (c) 17:00 on 02-09-2011.

A comparison between the filtered analytical approximation of the measured wave and the output from the CFD model can be seen in Figure 6. Since the model starts from a steady state, there is no correlation between the two waves in the initial stages of the simulation. However, after this stage, the two waves are found to be in very good agreement in terms of both frequency and amplitudes with a coefficient of determination, R^2, for the wave beginning at 10:30 on 17-12-2010, 4:30 on 04-10-2010 and 17:00 on 02-09-2011, of 80, 88.1 and 92.2, respectively. It is also observed

Please cite this article as: Finnegan W., Goggins J., 'Linear irregular wave generation in a numerical wave tank'. *Applied Ocean Research* 52 (2015) 188–200. DOI:10.1016/j.apor.2015.06.006

that the CFD model tends to smoothen out any dramatic changes in the elevation. In other words, it tends to replicate low frequency, high amplitude waves better than high frequency, low amplitude waves. Since the amplitude of the irregular wave is a summation of both high and low frequency waves, this may also have an effect on the accuracy of the model. Examples of this can be seen after 140 seconds in Figure 6(a) and after 100 seconds in Figure 6(b) where the CFD model underestimates the amplitude of the waves.

This analytical wave is then used to generate the input wave, given in Eqn. (15), and the corresponding horizontal and vertical water particle velocities, given in Eqn. (16) and Eqn. (17), respectively, which are to be inputted into the CFD model. In each model, the numerical wave is measured at a distance of 200 m from the input boundary. A set of wave profiles along the numerical wave tank model are shown in Figure 8 at different time-steps, for the simulation of the wave record beginning at 10:30 on 17-12-2010. The first wave profile is at 155.4 seconds and the others are at equal intervals of 3 seconds. This set of wave profiles is an example of how waves of different frequencies move at different speeds as the two smaller peaks after the main peak are moving slower relative to the main peak. This is a further reinforcement of the need for the $k_{0,n}x$ term, in Eqn. (14), when deriving the CFD input wave.

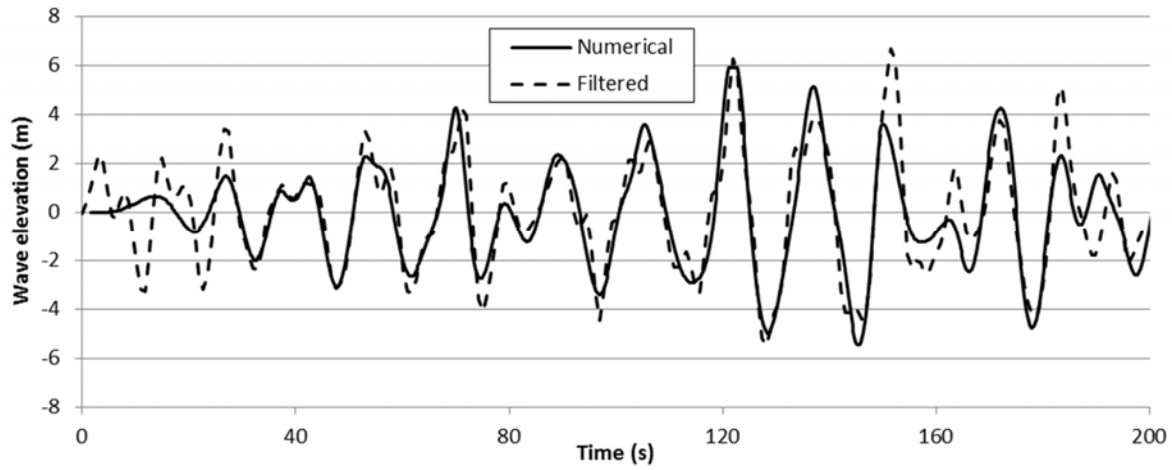

(a)

Please cite this article as: Finnegan W., Goggins J., 'Linear irregular wave generation in a numerical wave tank'. *Applied Ocean Research* 52 (2015) 188–200. DOI:10.1016/j.apor.2015.06.006

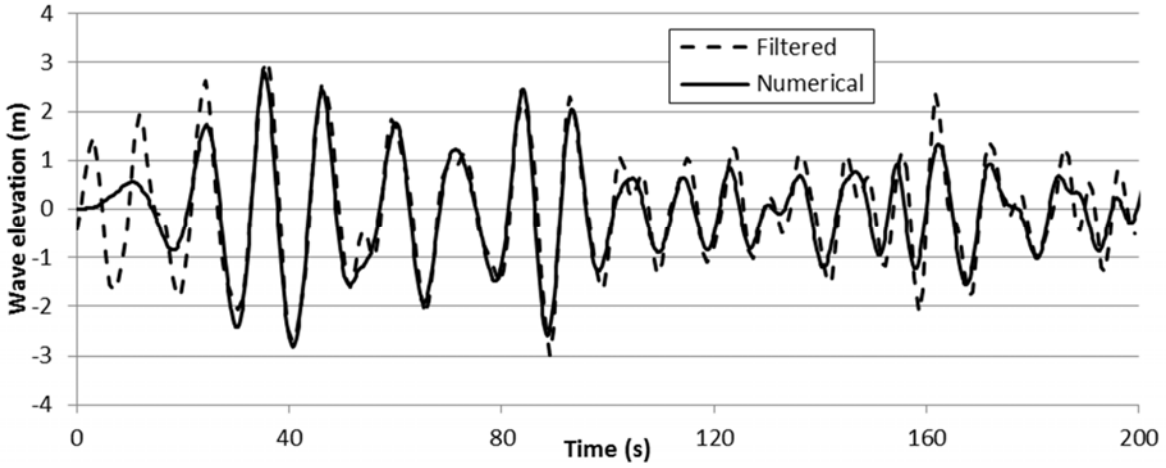

(b)

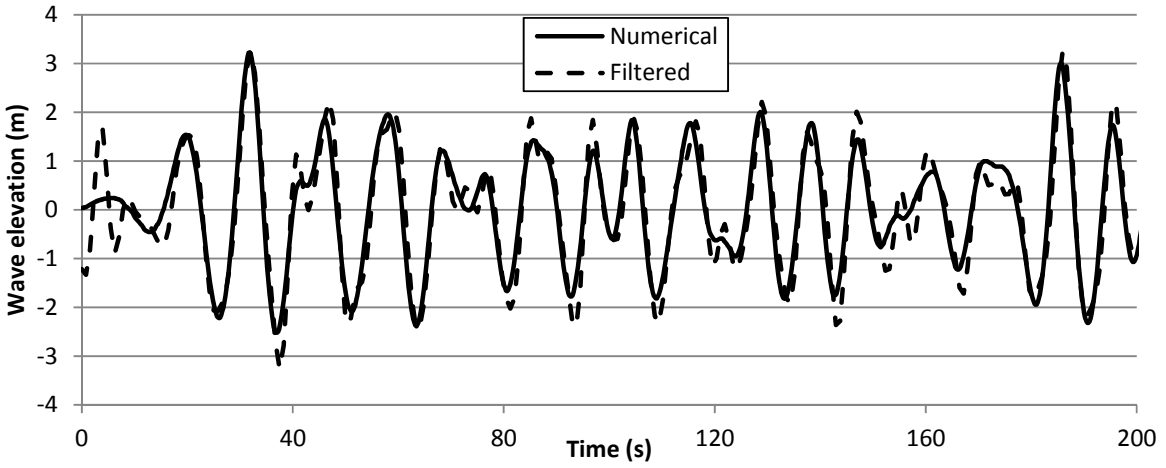

(c)

Figure 6: Comparison between the filtered analytical approximation wave and the output wave from the CFD model beginning at: (a) 10:30 on 17-12-2010 (b) 4:30 on 04-10-2010 and (c) 17:00 on 02-09-2011.

The absolute water particle velocity profile below the wave, at 200 m from the input boundary, for the filtered analytical approximation wave and the output wave from the CFD model are compared at three time steps, t = 80 s, 130 s and 150 s (Figure 7). The absolute water particle velocity for the filtered analytical approximation wave is calculated using Airy's linear wave theory, using Eqn.

Please cite this article as: Finnegan W., Goggins J., 'Linear irregular wave generation in a numerical wave tank'. *Applied Ocean Research* 52 (2015) 188–200. DOI:10.1016/j.apor.2015.06.006

(16) and (17). The velocity profile is given from the base to a height of 75m. Since the SWL is at a height of 70m from the base, large discrepancies can be seen between the filtered analytical approximation wave and the output wave from the CFD model above a height of 65m from the base. However, the velocity profiles are in very good agreement below 65m from the base, which gives good confidence in the numerical model.

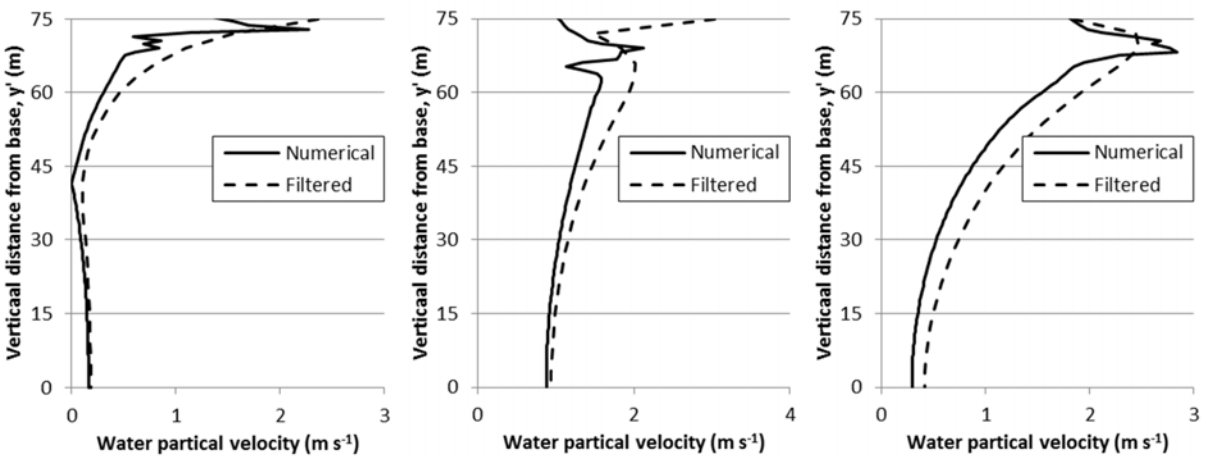

t = 80 s *t* = 130 s *t* = 180 s

(a)

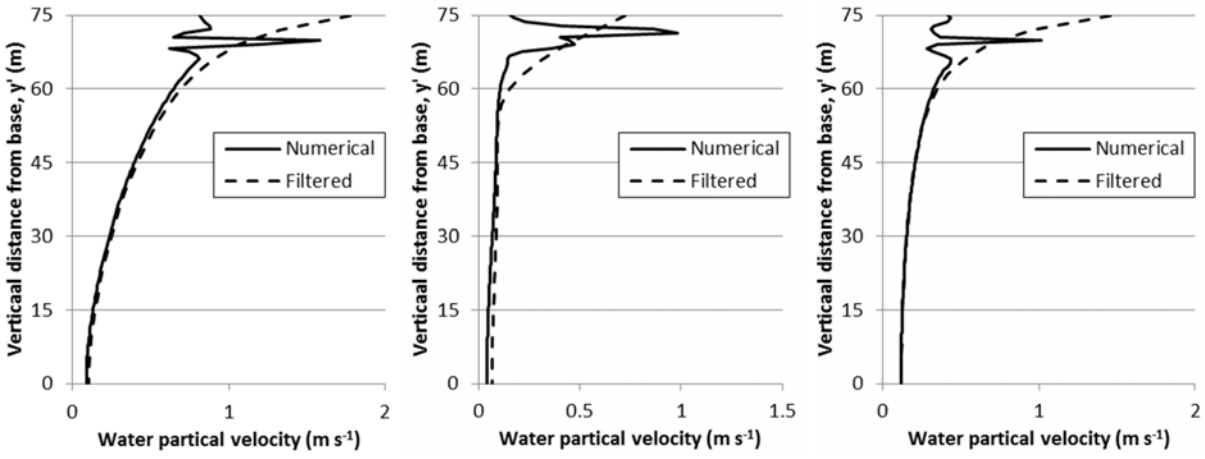

t = 80 s *t* = 130 s *t* = 180 s

(b)

Please cite this article as: Finnegan W., Goggins J., 'Linear irregular wave generation in a numerical wave tank'. *Applied Ocean Research* 52 (2015) 188–200. DOI:10.1016/j.apor.2015.06.006

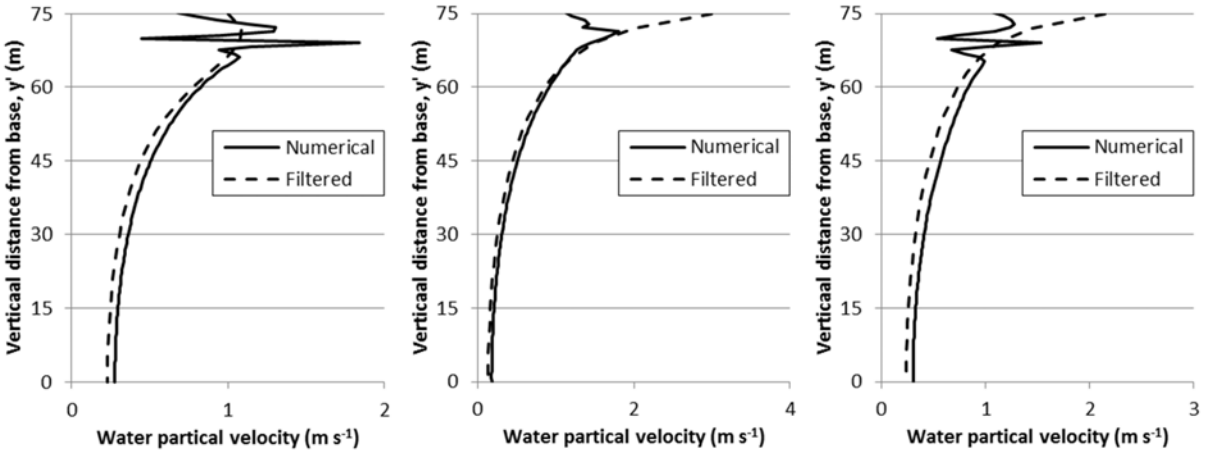

t = 80 s *t* = 130 s *t* = 180 s

(c)

Figure 7: Comparison between the absolute water particle velocities below the filtered analytical approximation wave and the output wave from the CFD model at three time steps, *t* = 80 s, 130 s and 150 s, beginning at: (a) 10:30 on 17-12-2010 (b) 4:30 on 04-10-2010 and (c) 17:00 on 02-09-2011.

Please cite this article as: Finnegan W., Goggins J., 'Linear irregular wave generation in a numerical wave tank'. *Applied Ocean Research* 52 (2015) 188–200. DOI:10.1016/j.apor.2015.06.006

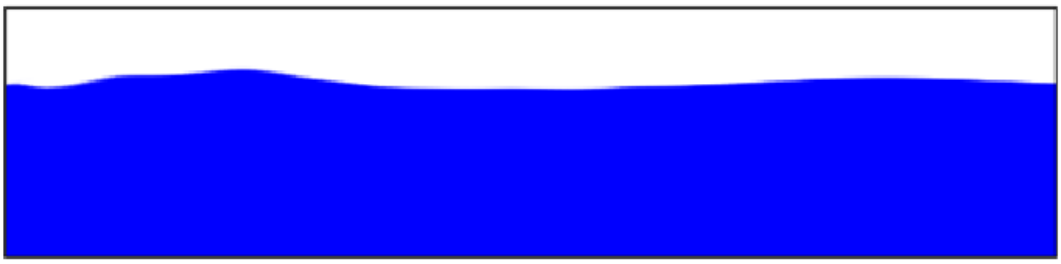

(a)

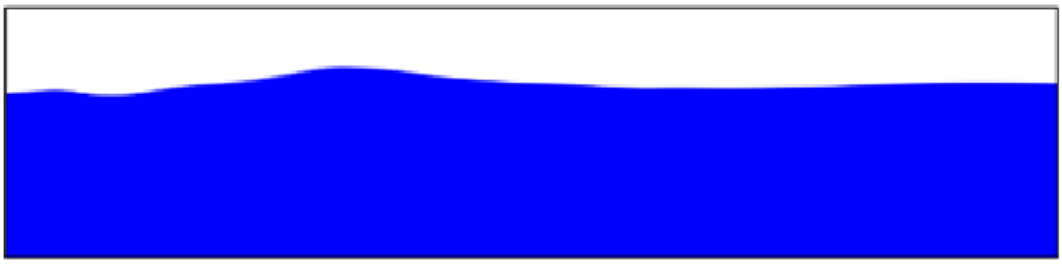

(b)

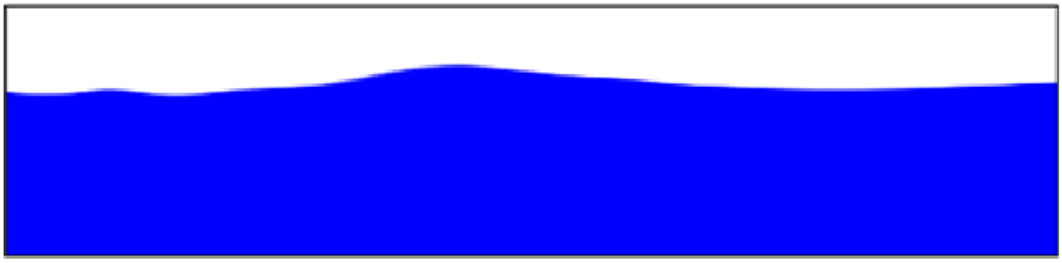

(c)

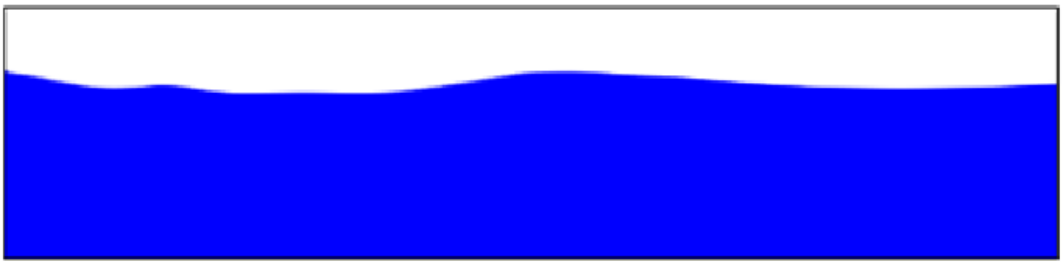

(d)

Figure 8: Longitudinal wave profile along the full length of the wave tank for different time-steps for the simulation of the wave record beginning at 10:30 on 17-12-2010. (a) beginning at 115.4 s and the subsequent in equal 4 second time intervals (i.e. (b) at 118.4 s, (c) at 121.4 s and (d) at 124.4 s).

Please cite this article as: Finnegan W., Goggins J., 'Linear irregular wave generation in a numerical wave tank'. *Applied Ocean Research* 52 (2015) 188–200. DOI:10.1016/j.apor.2015.06.006

The final part of the analysis is to calculate the wave energy spectrum of the output wave from the CFD model. A FFT is performed on the output wave from the CFD model and, using Eqn. (10), the wave energy spectrum can be calculated. This wave energy spectrum is then compared to the wave energy spectrum of the original measured wave, which can be seen in Figure 9. Again, the two spectra match very well in terms of frequency. However, there is a large discrepancy in the amplitude of the spectrum with dominant amplitudes at the peak frequencies within the numerical model. This, in turn, would increase the significant wave height of the resultant irregular wave. This is to be expected as there was an increase in the amplitude of the peaks in the filtered analytical irregular wave approximation compared to the measured wave, which is evident in Figure 5, and this approximation was used in deriving the numerical wave. However, this error may be reduced by reducing the amplitude of the linear wave at the peak frequency for the filtered analytical irregular wave approximation. Furthermore, there are discrepancies at high frequencies, generally greater than 0.15 s^{-1}, but these would not have a significant effect on the irregular wave elevation.

The analysis in this section was performed using a DELL Latitude E5540, which has a 4th gen Intel Core i5-4300U processor (1.9GHz, 3M Cache). The 250 second run took approximately 300 minutes, using the *'Serial'* run mode option within the ANSYS-CFX Solver Manager, to complete.

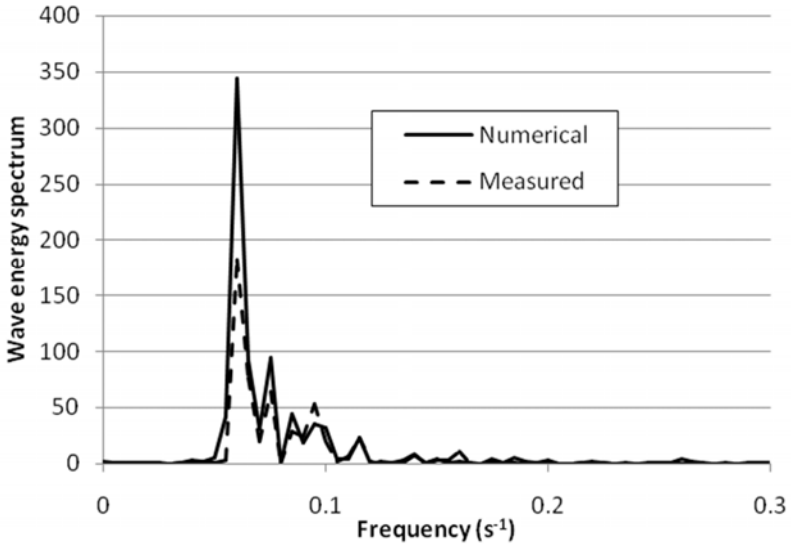

Please cite this article as: Finnegan W., Goggins J., 'Linear irregular wave generation in a numerical wave tank'. *Applied Ocean Research* 52 (2015) 188–200. DOI:10.1016/j.apor.2015.06.006

(a)

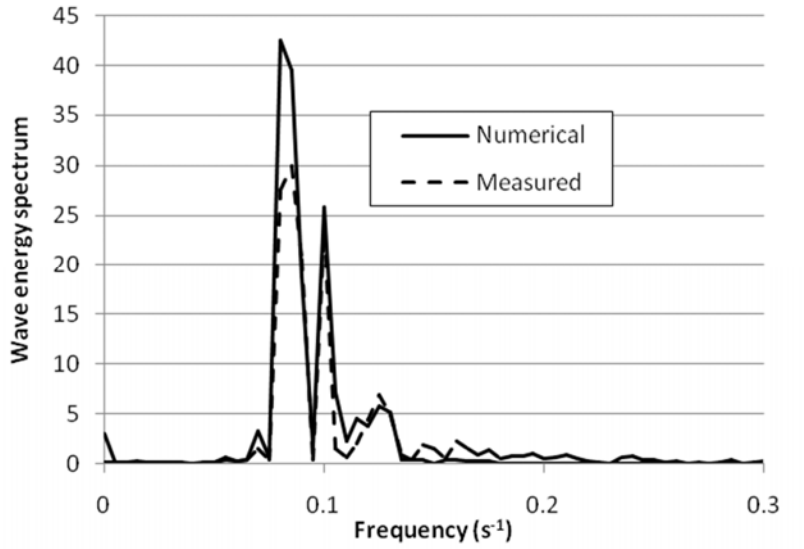

(b)

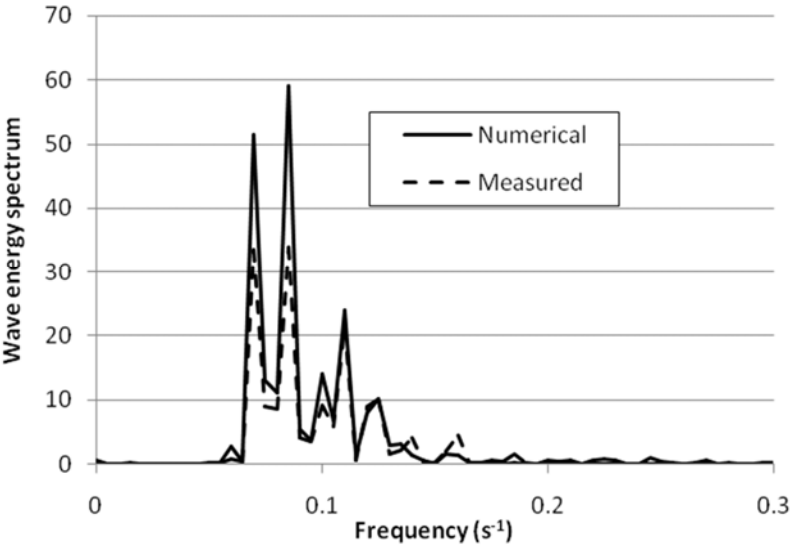

(c)

Figure 9: Comparison between the wave energy spectrum of the measured wave and output wave from CFD model beginning at: (a) 10:30 on 17-12-2010 (b) 4:30 on 04-10-2010 and (c) 17:00 on 02-09-2011.

Please cite this article as: Finnegan W., Goggins J., 'Linear irregular wave generation in a numerical wave tank'. *Applied Ocean Research* 52 (2015) 188–200. DOI:10.1016/j.apor.2015.06.006

4. Interaction of a structure with a linear irregular water wave

The next stage of the analysis is to introduce a structure into the model in order to explore the interaction of the structure with a linear irregular water wave. In this study, an infinitely long rectangular prism is employed as the structure in order to analyse the accuracy of the model's prediction of the heave motion dynamic response of a structure in the presence of a linear irregular wave. The infinitely long rectangular prism has a width of 30 m, a draft of 15 m with a total structural height of 20 m, and its centre is at a distance of 200 m from the inflow boundary.

The *'Rigid Body'* fluid-structure interaction feature of ANSYS CFX [21] is used to model the floating structure. The floating structure is defined by collection of 2D regions that form its faces (in this case, a section is cut from the fluid domain to generate these 2D regions) and specified within the 'Rigid Body' feature. Using this method, the rigid body itself does not need to be meshed. Mesh motion is used to move the mesh on the rigid body faces in accordance with the solution of the rigid body equations of motion, which is determined by a fully integrated and implicit six-degree-of-freedom rigid body solver within ANSYS CFX. The feature also requires a number of properties of the structure, including centre of gravity, moments of inertia, translational and rotational degrees of freedom and either initial velocity or initial acceleration components. In this analysis, the movement of the structure is restricted to two-degrees-of-freedom; the heave, or vertical, motion and the pitch, or rotation about the z-axis, motion. Additionally, external forces and torques may be defined. Furthermore, the initial velocity components of the structure are set to zero and its centre of gravity is set equal to its initial centre of buoyancy.

It may be noted that when the structure is introduced into the model, additional mesh refinement is required around the structure. The *'Sphere of Influence'* mesh refinement method is used and, therefore, the total number of elements in the mesh is increased to 40000. Further adaptions to the model are also required to ensure the robustness of the model during the analysis. At the beginning of the simulation, a ramp time-step is introduced, where the time-step is reduced from 0.1 s to 0.025 s for the first second, or first 40 time-steps, of the simulation. In addition, defined mesh stiffness is included in the model, which is the inverse of the volume of the element. Therefore,

Please cite this article as: Finnegan W., Goggins J., 'Linear irregular wave generation in a numerical wave tank'. *Applied Ocean Research* 52 (2015) 188–200. DOI:10.1016/j.apor.2015.06.006

the smaller elements have greater mesh stiffness and, thus, are less likely to fold or invert during the remeshing, which will cause the simulation to crash or fail.

The interaction between a linear irregular ocean wave and a structure, which includes the wave profile and the dynamic response of the structure, over a number of time-steps, can be seen in Figure 10. Figure 10 (a) at 128.4 s of the simulation is replicating the wave record beginning at 17:00 on 02-09-2011, while Figure 10 (b)-(d) are in equal 4 second subsequent time intervals.

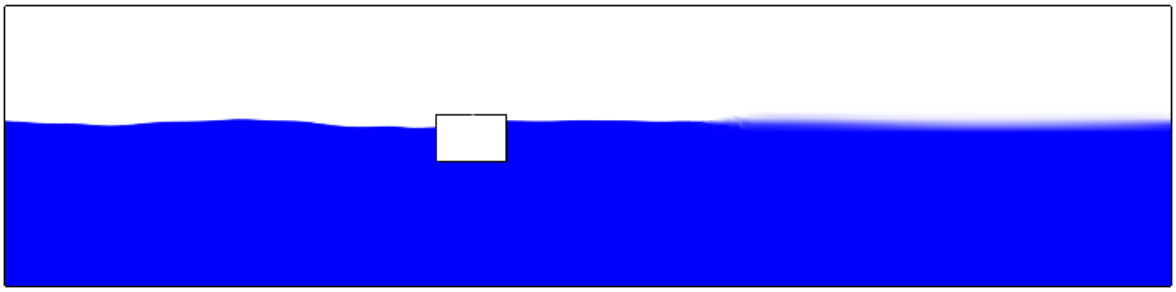

(a)

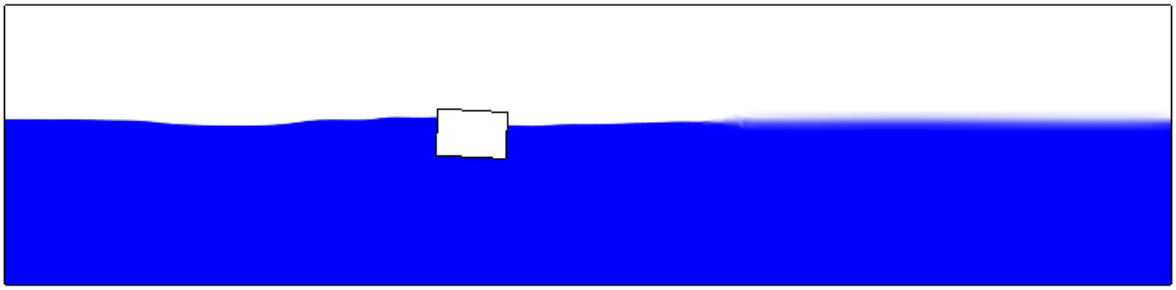

(b)

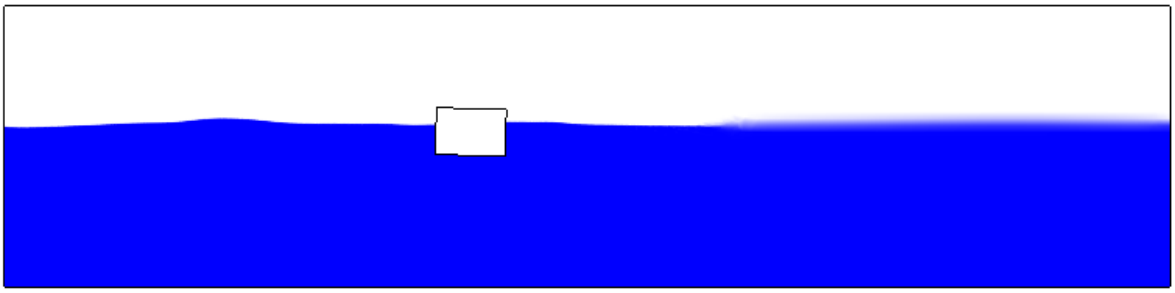

(c)

Please cite this article as: Finnegan W., Goggins J., 'Linear irregular wave generation in a numerical wave tank'. *Applied Ocean Research* 52 (2015) 188–200. DOI:10.1016/j.apor.2015.06.006

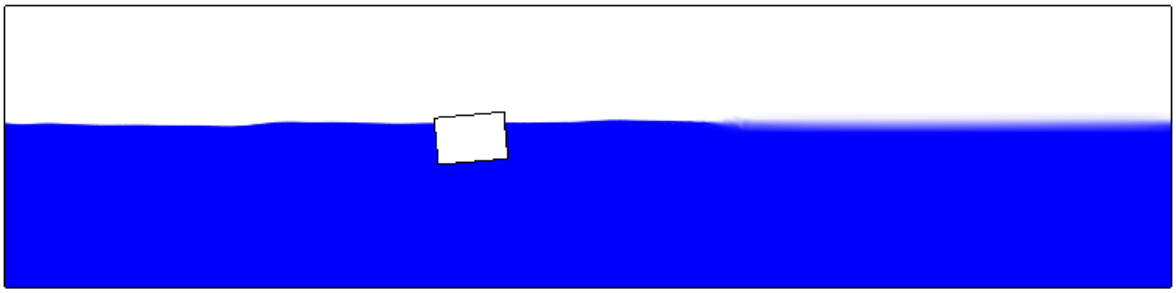

(d)

Figure 10: Wave profile and dynamic response of the structure for different time steps beginning at 17:00 on 02-09-2011. (a) beginning at 128.4 s and the subsequent in equal 4 second time intervals (i.e. (b) at 132.4 s, (c) at 136.4 s and (d) at 140.4 s).

Furthermore, in order to assess the accuracy of the model, the heave motion dynamic response from the NWT is compared to a simple analytical solution derived from the hydrodynamic analysis of the structure. The hydrodynamic analysis is performed using the commercial boundary element method software package ANSYS AQWA [27]. A parametric study was performed to determine the length of the prism required to accurately replicate the normalised dynamic response of the infinitely long structure to beam sea conditions. From this, a length of 100 m was deemed sufficient. The normalised dynamic response, $\hat{u}$, and the phase angle, β, is shown graphically in Figure 11. It is noted in Figure 11 that after the initial stage, the phase angle does not behave the same in the NWT as for a single degree of freedom system. This is a result of a contribution from the pitch motion dynamic response of the structure that alters the phase angle of the heave motion dynamic response. The dynamic response is determined analytically, u, in the time-domain, using the following expression:

$$u(t) = \sum_{n=1}^{N} A_n \hat{u}_n \, cos(-\omega_n t - \varepsilon'_n - \beta_n) \tag{18}$$

A comparison of the dynamic response of the structure from the NWT model and the analytical solution, given in Eqn. (18), is shown in well in terms of frequency, but there is a difference in the amplitude of the response. There is a large discrepancy in the initial part of the simulation between the two solutions, since the NWT model starts at a steady state. However, the two solutions begin

Please cite this article as: Finnegan W., Goggins J., 'Linear irregular wave generation in a numerical wave tank'. *Applied Ocean Research* 52 (2015) 188–200. DOI:10.1016/j.apor.2015.06.006

to converge for the second half of the record. This difference may be attributed to the effects of position-change and inclination situation of the floating structure causing the wetted surface to change throughout the run. This effect on the hydrodynamic load on the floating structure is taken into consideration when using the CFD coupling model, while it is ignored in the analytical solution. In other words, the wave forces in the CFD model are integrated on wetted surface over the instantaneous position of the floating structure while the analytical solution neglects the change of the wet surface of the floating structure. Additionally, the viscous non-linearties present in the numerical model for a wave tank around the wall, or hull, of the structure itself causing increased damping forces which are not present in the hydrodynamic analysis model, may contribute to the difference between the CFD model and the analytical solution.

Similar to Section 3, the analysis in this section was performed using a DELL Latitude E5540, which has a 4th gen Intel Core i5-4300U processor (1.9GHz, 3M Cache). However, the 250 second run took approximately 2600 minutes, using the *'Serial'* run mode option within the ANSYS-CFX Solver Manager, to complete. The longer solving time is a result of an increased number of elements within the mesh and a remeshing requirement at each time-step as a result of the moving *'Rigid Body'* boundaries.

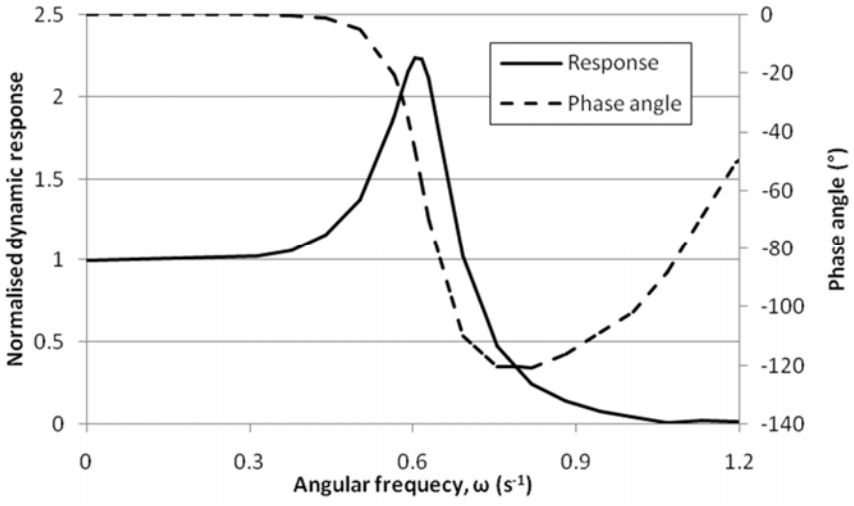

Figure 11: The normalised heave motion dynamic response and associated phase angle from the hydrodynamic analysis of the structure.

Please cite this article as: Finnegan W., Goggins J., 'Linear irregular wave generation in a numerical wave tank'. *Applied Ocean Research* 52 (2015) 188–200. DOI:10.1016/j.apor.2015.06.006

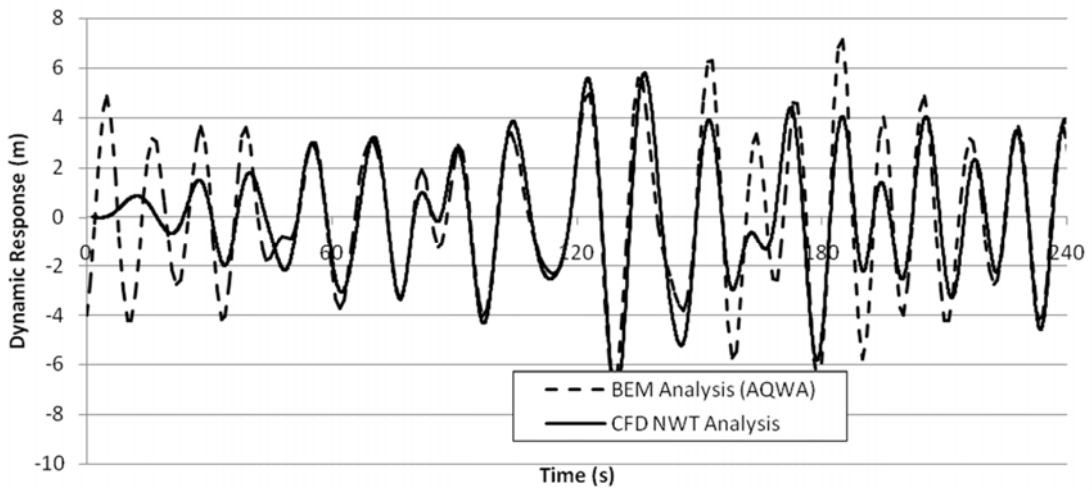

(a)

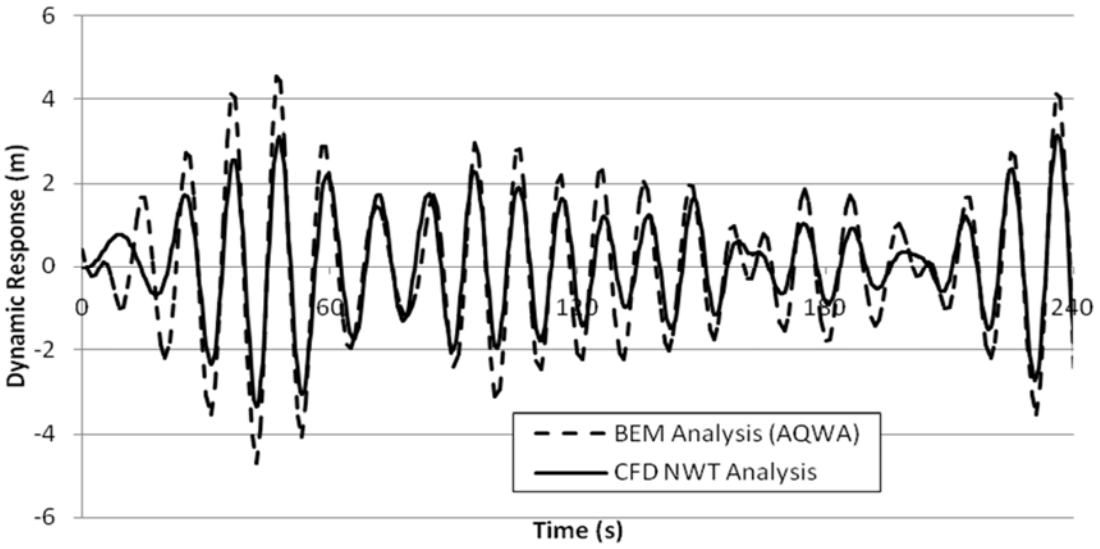

(b)

Please cite this article as: Finnegan W., Goggins J., 'Linear irregular wave generation in a numerical wave tank'. *Applied Ocean Research* 52 (2015) 188–200. DOI:10.1016/j.apor.2015.06.006

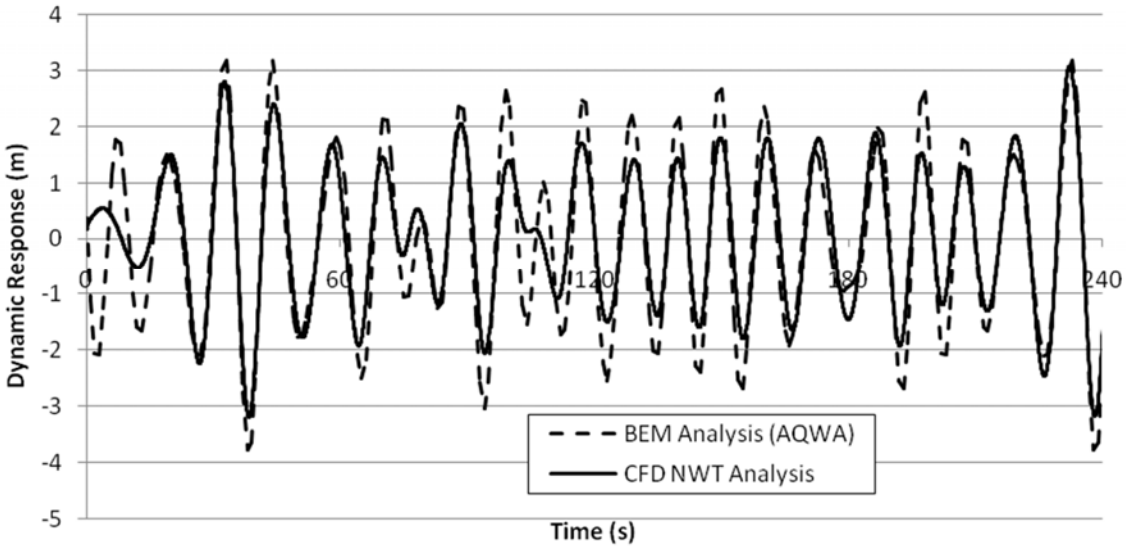

(c)

Figure 12: Comparison of the heave motion dynamic response of the rectangular prism from the CFD NWT analysis and analytical hydrodynamic analysis beginning at: (a) 10:30 on 17-12-2010 (b) 4:30 on 04-10-2010 and (c) 17:00 on 02-09-2011.

5. Discussion and conclusions

In this paper, a numerical model for a wave tank that can accurately mimic real ocean waves is developed. It is clear from this analysis that real ocean wave conditions can be modelled accurately and relative inexpensively in comparison to physical model testing. Furthermore, numerical modelling is used to its maximum by employing full scale measured data and replicating it in a full-scale numerical wave tank. The ability of the model to accurately model measured ocean waves and their interaction with a floating structure is the novel aspect here.

The model developed in Finnegan and Goggins [16] is extended in order to generate linear irregular waves, which can be used to model real ocean waves. An adaption, of note, to the model is the use of a laminar turbulence model in the current study, as the turbulence model used has an effect on the numerical procedure. The detailed methodology for generating linear irregular waves has been used to replicate wave records measured at AMETS. In order to demonstrate the robustness of the methodology, three different wave records are analysed throughout the chapter.

Please cite this article as: Finnegan W., Goggins J., 'Linear irregular wave generation in a numerical wave tank'. *Applied Ocean Research* 52 (2015) 188–200. DOI:10.1016/j.apor.2015.06.006

A comparison between the filtered analytical approximation of the measured wave and the output from the CFD model is analysed. Since the model starts from a steady state, there is no correlation between the two waves in the initial stages of the simulation. However, after this stage, the two waves are found to be in very good agreement in terms of both frequency and amplitudes with a coefficient of determination, R^2, ranging from 80 to 92.2. It is also observed that the CFD model tends to smoothen out any dramatic changes in the elevation. In other words, it tends to replicate low frequency, high amplitude waves better than high frequency, low amplitude waves. Additionally, the absolute water particle velocity profile below the wave, at 200 m from the input boundary, for the filtered analytical approximation wave and the output wave from the CFD model are compared at three time steps, t = 80 s, 130 s and 150 s and are in very good agreement below 65m from the base, which gives good confidence in the numerical model.

A rectangular floating prism is introduced into the model in order to explore the accuracy of wave-structure interaction prediction. A comparison of the heave motion dynamic response of the structure from the NWT model and the analytical solution indicates that the two solutions were in good agreement. In particular, both solutions match very well in terms of frequency. However, there is a difference in the peak amplitude of the response. This difference may be attributed to the viscous non-linearties present in the numerical model for a wave tank around the wall, or hull, of the structure itself causing increased damping forces, which are not present in the hydrodynamic analysis model. There is a large discrepancy in the initial part of the simulation between the two solutions, since the NWT model starts at a steady state. However, the two solutions begin to converge for the second half of the record.

In this paper, the analysis is restricted to two-degrees-of-freedom; the heave, or vertical, motion and the pitch, or rotation about the z-axis, motion. Nonetheless, large-amplitude sway motions may also be modelled using the methodology described. However, this was outside the scope of the study but may be included in a future study.

The methodology detailed in this paper provides the user with a very inexpensive method of performing wave-structure interaction in realistic ocean conditions, without the need for sea trials. The use of the numerical model is maximised here as no scaling is introduced, therefore a more realistic model and structure response is presented. This methodology also provides a far more

Please cite this article as: Finnegan W., Goggins J., 'Linear irregular wave generation in a numerical wave tank'. *Applied Ocean Research* 52 (2015) 188–200. DOI:10.1016/j.apor.2015.06.006

realistic estimate of the energy extraction ability of a wave energy converter compared to the use of a linear regular wave tank.

Acknowledgements

The first author would like to acknowledge the financial support from the National University of Ireland under the College of Engineering & Informatics Postgraduate Fellowship. Furthermore, the authors would like to express their gratitude to the Marine Institute for supplying the wave-rider data for the AMETS and the Irish centre for high-end computing (ICHEC) for the computation processing power provided. Part of this material is based upon works supported by the Science Foundation Ireland under Grant No. 12/RC/2302 through MaREI, the national centre for Marine Renewable Energy Ireland.

References:

[1] Kim MH, Niedzwecki JM, Roesset JM, Park JC, Hong SY, Tavassoli A. Fully Nonlinear Multidirectional Waves by a 3-D Viscous Numerical Wave Tank. Journal of Offshore Mechanics and Arctic Engineering. 2001;123:124-33.

[2] Boo SY. Linear and nonlinear irregular waves and forces in a numerical wave tank. Ocean Engineering. 2002;29:475-93.

[3] Turnbull MS, Borthwick AGL, Eatock Taylor R. Wave-structure interaction using coupled structured-unstructured finite element meshes. Applied Ocean Research. 2003;25:63-77.

[4] Koo W, Kim MH. Freely floating-body simulation by a 2D fully nonlinear numerical wave tank. Ocean Engineering. 2004;31:2011-46.

[5] Park JC, Uno Y, Sato T, Miyata H, Chun HH. Numerical reproduction of fully nonlinear multi-directional waves by a viscous 3D numerical wave tank. Ocean Engineering. 2004;31:1549-65.

[6] Wu GX, Hu ZZ. Simulation of nonlinear interactions between waves and floating bodies through a finite-element-based numerical tank. Proceedings of the Royal Society of London Series A: Mathematical, Physical and Engineering Sciences. 2004;460:2797-817.

[7] Hadzic I, Hennig J, Peric M, Xing-Kaeding Y. Computation of flow-induced motion of floating bodies. Applied Mathematical Modelling. 2005;29:1196-210.

[8] Sriram V, Sannasiraj SA, Sundar V. Simulation of 2-D nonlinear waves using finite element method with cubic spline approximation. Journal of Fluids and Structures. 2006;22:663-81.

Please cite this article as: Finnegan W., Goggins J., 'Linear irregular wave generation in a numerical wave tank'. *Applied Ocean Research* 52 (2015) 188–200. DOI:10.1016/j.apor.2015.06.006

[9] Ning DZ, Teng B. Numerical simulation of fully nonlinear irregular wave tank in three dimension. International Journal for Numerical Methods in Fluids. 2007;53:1847-62.

[10] Agamloh EB, Wallace AK, von Jouanne A. Application of fluid-structure interaction simulation of an ocean wave energy extraction device. Renewable Energy. 2008;33:748-57.

[11] Lal A, Elangovan M. CFD Simulation and Validation of Flap Type Wave-Maker. World Academy of Science, Engineering and Technology. 2008;46:7.

[12] Ning DZ, Teng B, Eatock Taylor R, Zang J. Numerical simulation of non-linear regular and focused waves in an infinite water-depth. Ocean Engineering. 2008;35:887-99.

[13] Liang X, Yang J, Li J, Xiao L, Li X. Numerical Simulation of Irregular Wave-Simulating Irregular Wave Train. Journal of Hydrodynamics. 2010;22:537-45.

[14] Elangovan M. Simulation of Irregular Waves by CFD. World Academy of Science, Engineering and Technology 2011;55.

[15] Yan H, Liu Y. An efficient high-order boundary element method for nonlinear wave-wave and wave-body interactions. Journal of Computational Physics. 2011;230:402-24.

[16] Finnegan W, Goggins J. Numerical simulation of linear water waves and wave-structure interaction. Ocean Engineering. 2012;43:23-31.

[17] Yu Y-H, Li Y. Reynolds-Averaged Navier–Stokes simulation of the heave performance of a two-body floating-point absorber wave energy system. Computers & Fluids. 2013;73:104-14.

[18] Contento G. Numerical wave tank computations of nonlinear motions of two-dimensional arbitrarily shaped free floating bodies. Ocean Engineering. 2000;27:531-56.

[19] Marine Institute. Marine Institute. 2012.

[20] Goggins J, Finnegan W. Shape optimisation of floating wave energy converters for a specified wave energy spectrum. Renewable Energy. 2014;71:208-20.

[21] ANSYS Inc. ANSYS CFX, Release 12.1. 2009.

[22] Versteeg HK, Malalasekera W. An Introduction to Computational Fluid Dynamics, The Finite Volume Method. Essex, England: Prentice Hall; 1995.

[23] Kim CH. Nonlinear Waves and Offshore Structures: World Scientific Publishing Co. Pte. Ltd.; 2008.

[24] Zhao Y-p, Xu T-j, Dong G-h, Li Y-c. Numerical simulation of a submerged gravity cage with the frame anchor system in irregular waves. Journal of Hydrodynamics, Ser B. 2010;22:433-7.

[25] Dong G-H, Xu T-J, Zhao Y-P, Li Y-C, Gui F-K. Numerical simulation of hydrodynamic behavior of gravity cage in irregular waves. Aquacultural Engineering. 2010;42:90-101.

[26] Xu T-J, Dong G-H, Zhao Y-P, Li Y-C, Gui F-K. Analysis of hydrodynamic behaviors of gravity net cage in irregular waves. Ocean Engineering. 2011;38:1545-54.

[27] ANSYS Inc. ANSYS AQWA, Release 13. 13 ed2010.